Preprint typeset in JHEP style - HYPER VERSION

Confronting the relaxation mechanism for a large cosmological constant with observations

Spyros Basilakos[a,b], **Florian Bauer**[a,c], **Joan Solà**[a,c]

[a] *High Energy Physics Group, Dept. ECM, Univ. de Barcelona, Av. Diagonal 647, E-08028 Barcelona, Catalonia, Spain*

[b] *Academy of Athens, Research Center for Astronomy and Applied Mathematics, Soranou Efesiou 4, 11527, Athens, Greece*

[c] *Institut de Ciències del Cosmos, Univ. de Barcelona*

E-Mails: svasil@academyofathens.gr, fbauerphysik@eml.cc, sola@ecm.ub.es

Abstract: In order to deal with a large cosmological constant a relaxation mechanism based on modified gravity has been proposed recently. By virtue of this mechanism the effect of the vacuum energy density of a given quantum field/string theory (no matter how big is its initial value in the early universe) can be neutralized dynamically, i.e. without fine tuning, and hence a Big Bang-like evolution of the cosmos becomes possible. Remarkably, a large class $\{F_m^n\}$ of models of this kind, namely capable of dynamically adjusting the vacuum energy irrespective of its value and size, has been identified. In this paper, we carefully put them to the experimental test. By performing a joint likelihood analysis we confront these models with the most recent observational data on type Ia supernovae (SNIa), the Cosmic Microwave Background (CMB), the Baryonic Acoustic Oscillations (BAO) and the high redshift data on the expansion rate, so as to determine which ones are the most favored by observations. We compare the optimal relaxation models F_m^n found by this method with the standard or concordance ΛCDM model, and find that some of these models may appear as almost indistinguishable from it. Interestingly enough, this shows that it is possible to construct viable solutions to the tough cosmological fine tuning problem with models that display the same basic phenomenological features as the concordance model.

Keywords: dynamical dark energy, cosmological constant.

Contents

1. Introduction

Current observations [1, 2] indicate that the cosmological constant (CC) Λ, or equivalently the vacuum energy density $\rho_\Lambda = \Lambda/(8\pi G_N)$, is non-vanishing and positive, and of the order of $\rho_\Lambda^0 \sim 10^{-47}\,\mathrm{GeV}^4$. This value is close to 70% of the present critical energy density in our universe, ρ_c^0, and therefore is very small in Particle Physics units (being equivalent to having a mass density of a few protons per cubic meter). In itself, the inclusion of the tiny value ρ_Λ^0 as a cosmological term in the gravity action would not be a problem. However, the modern fundamental physical theories suggest that large contributions to the classical CC parameter (in particular those sourced by quantum fluctuations of the matter fields) are induced, resulting into a huge initial CC value of order $|\rho_\Lambda^i| \sim M_X^4$ which is fed into the cosmos already in the phase transitions of the early universe, with M_X in the range between the electro-weak (EW) scale $\sim 100\,\mathrm{GeV}$ and the Planck scale $\sim 10^{19}\,\mathrm{GeV}$. Even if "only" the EW scale of the Standard Model (SM) of Particle Physics would be involved in the induced CC value, the discrepancy with respect to the observed value ρ_Λ^0 entails 55 orders

of magnitude[1]. This is of course preposterous. Despite none of these vacuum contributions is directly supported by experimental evidence yet, there is hardly a theory beyond the SM that does not come with a large value of $\Lambda = 8\pi\, G_N\, \rho_\Lambda$ induced by the huge vacuum energy density ρ_Λ predicted by the theory and whose origin may be both from the zero point vacuum fluctuations of the matter fields as well as from the spontaneous symmetry breaking of the gauge theories. In principle, all models with scalar fields (in particular the SM with its Higgs boson sector) end up with a large vacuum energy density ρ_Λ associated to their potentials. For example, from the SM Higgs potential we expect $\rho_\Lambda \sim 10^8$ GeV^4, which explains the aforementioned 55 orders of magnitude discrepancy and corresponding $55^{\rm th}$ digit fine tuning CC problem. The huge hierarchy between the predicted and the observed CC, the so-called "old CC problem" [3], is one of the biggest mysteries of theoretical physics of all times. To avoid removing the huge initial value of the vacuum energy density ρ_Λ^i by hand with an extremely fine tuned counterterm [2] (giving the theory a very unpleasant appearance), alternative dark energy models have been suggested. Typically, these models replace the large CC by a dynamical energy source [see [5] and references therein]. This seems reasonable for describing the observed late-time acceleration, but generally it still requires that the large CC has been removed somehow. In the end, it means that a fine tuned counterterm has been tacitly assumed [6].

It is encouraging that time-varying vacuum energy models inspired by the principles of QFT can be suggested and may hopefully provide an alternative and more efficient explanation for the dynamical nature of the vacuum energy [7]. Recently the analysis of some well motivated models of this kind versus the observations has shown that their phenomenological status is perfectly reasonable and promising [8, 9] – see also the recent works [10]. However, in order to solve the old CC problem in this context, we need to focus on models that dynamically counteract the large initial ρ_Λ^i. The idea, in a nutshell, is: 1) to obtain an effective $\rho_{\Lambda{\rm eff}}(t)$ (the measured one) which satisfies $|\rho_{\Lambda{\rm eff}}(t)| \ll |\rho_\Lambda^i|$ at all times t and without fine-tuning; 2) to insure that $\rho_{\Lambda{\rm eff}}(t)$ preserves the standard cosmic evolution (i.e. the correct sequence of radiation, matter and dark energy dominated epochs); and finally 3) to make sure that $\rho_{\Lambda{\rm eff}}(t)$ is able to reproduce the measured value of the vacuum energy at present, $\rho_{\Lambda{\rm eff}}(t_0) \sim \rho_\Lambda^0$, again without fine-tuning. Only in this way we can guarantee a low-curvature universe similar to ours, namely $R = 8\pi\, G_N \rho_{\Lambda{\rm eff}} \sim 8\pi\, G_N \rho_c^0 \sim H_0^2$, with $H_0 \sim 10^{-42}$ GeV the current Hubble rate. The question of course is: is that program really possible?

Obviously, in order to follow this road in a successful way it is necessary to go beyond the common dark energy models and face a class of scenarios where the large CC is not hidden under the rug, so to speak, but rather it is permanently considered as a fundamental ingredient of the overall theory of the cosmos. In this work, we analyze a class (probably not unique) of models operating along this line, namely the CC relaxation mechanism based on

[1] Let us note that the QCD scale of the strong interactions, $\Lambda_{\rm QCD} \sim 100$ MeV, could also trigger an induced vacuum energy density $\rho_\Lambda \sim \Lambda_{\rm QCD}^4$, which would then be roughly 43 orders of magnitude larger than ρ_Λ^0. We have nevertheless taken the EW value because it is larger and is considered also as a robust fundamental scale in the structure of the SM of Particle Physics.

[2] See e.g. a detailed account of the old fine tuning CC problem in Sect. 2, and Appendix B, of Ref. [4].

$F(R,\mathcal{G})$ modified gravity [4, 11, 12]. These models are intimately related with the family of the so-called ΛXCDM models of the cosmic evolution [13] (in which X is generally *not* a scalar field, but an effective quantity in the equations of motion which derives from the complete structure of the effective action). They might also be connected with mechanisms based on matter with an inhomogeneous equation of state [14]. A first modified gravity approach implementing the relaxation mechanism was presented in [15]. Furthermore, a related model in the alternative Palatini formalism has been studied [16], too.

As stated, the class of models considered here is probably just a subset of a larger class of theories that can produce dynamical relaxation of the vacuum energy. Our work should ultimately be viewed as aiming at illustrative purposes only, i.e. as providing a proof of existence that one can construct explicitly a relaxation mechanism, if only in a moderately realistic form [3]. We cannot exclude that more sophisticated and efficient mechanisms can be eventually discovered which are much more realistic, but at the moment the $F(R,\mathcal{G})$ models serve quite well our illustrative purposes. They constitute a potentially important step in the long fighting of Theoretical Physics against the tough CC problem, especially in regard to the appalling fine tuning conundrum inherent to it. Additional work recently addressing the CC problem from various perspectives can be found e.g. in Refs. [18].

In contrast to late-time gravity modifications, in the relaxation mechanism an effective energy density $\rho_F(t)$ is permanently induced by the $F(R,\mathcal{G})$ modification to the standard gravity action, which counteracts dynamically (at any time of the postinflationary cosmic history) the effect of the large vacuum energy density ρ_Λ^i and provides the net value $\rho_{\Lambda\text{eff}} = \rho_\Lambda^i + \rho_F$ (presumably close to the observationally measured one ρ_Λ^0). As a result the universe has an expansion history similar, but not identical, to the concordance ΛCDM model. Therefore, it is important to investigate how the relaxation models perform with respect to observational constraints coming from the Cosmic Microwave Background (CMB) [1], type Ia supernovae (SNIa) [2], the Baryonic Acoustic Oscillations (BAO) [19] and the high redshift data on the expansion rate [20].

The paper is organized as follows: in Sect. 2 we discuss different aspects of the working principle of the CC relaxation mechanism in modified gravity. In Sect. 3 we present the numerical tools that we use to perform the statistical analysis, and in Sect. 4 we apply them to determine the optimal relaxation model candidates with a further insight in the details of the relaxation mechanism. In Sect. 5 we present predictions for the redshift evolution of the deceleration parameter and the effective equation of state, and compare with the ΛCDM. In the last section we deliver our conclusions. Finally, in an appendix we provide some useful formulae discussed in the text.

2. Vacuum relaxation in $F(R,\mathcal{G})$ modified gravity

The general form of the complete effective action of the cosmological model in terms of the

[3] Remember that in the past the dynamical adjustment of the CC was attempted through scalar field models [17], but later on a general no-go theorem was formulated against them [3]. Fortunately, this theorem can be circumvented by the relaxation mechanism, see [4] for details.

Ricci scalar R and the Gauss-Bonnet invariant $\mathcal{G}$ is given by

$$\mathcal{S} = \int d^4x \sqrt{|g|} \left[\frac{1}{16\pi G_N} R - \rho^i_\Lambda - F(R,\mathcal{G}) + \mathcal{L}_\phi \right], \tag{2.1}$$

where $\mathcal{L}_\phi$ denotes the Lagrangian of the matter fields. This action represents the Einstein-Hilbert action extended by the term $F(R,\mathcal{G})$ defining the modification of gravity. Moreover, we include all vacuum energy contributions from the matter sector in the large CC term ρ^i_Λ.

From the above action the modified Einstein equations are derived by the variational principle $\delta\mathcal{S}/\delta g^{ab} = 0$. They read

$$G^a_{\ b} = -8\pi G_N \left[\rho^i_\Lambda \, \delta^a_{\ b} + 2E^a_{\ b} + T^a_{\ b} \right], \tag{2.2}$$

with the Einstein tensor $G^a_{\ b} = R^a_{\ b} - \frac{1}{2}\delta^a_{\ b} R$, the cosmological term and the energy-momentum tensor $T^a_{\ b}$ of matter emerging from $\mathcal{L}_\phi$.

We describe the cosmological background by the spatially flat FLRW line element $ds^2 = dt^2 - a^2(t) d\vec{x}^{\,2}$ with the scale factor $a(t)$ and the cosmological time t. Accordingly, the curvature invariants $R = 6H^2(1-q)$ and $\mathcal{G} = -24H^4 q$ can be expressed in terms of the Hubble expansion rate $H = \dot{a}/a$ and the deceleration parameter $q = -\ddot{a}a/\dot{a}^2$. The tensor components in (2.2) are given by $G^0_{\ 0} = -3H^2$, $G^i_{\ j} = -\delta^i_{\ j}(2\dot{H} + 3H^2)$ and

$$E^0_{\ 0} = \frac{1}{2}\left[F - 6(\dot{H}+H^2)F^R + 6H\dot{F}^R - 24H^2(\dot{H}+H^2)F^{\mathcal{G}} + 24H^3\dot{F}^{\mathcal{G}} \right] \tag{2.3}$$

$$\begin{aligned} E^i_{\ j} = \frac{1}{2}\,\delta^i_{\ j} \Big[& F - 2(\dot{H}+3H^2)F^R + 4H\dot{F}^R + 2\ddot{F}^R \\ & -24H^2(\dot{H}+H^2)F^{\mathcal{G}} + 16H(\dot{H}+H^2)\dot{F}^{\mathcal{G}} + 8H^2\ddot{F}^{\mathcal{G}} \Big], \end{aligned} \tag{2.4}$$

where $F^Y \equiv \partial F/\partial Y$ stand for the partial derivatives of F with respect to $Y = R, \mathcal{G}$. The F-term induces the effective energy density $\rho_F = 2E^0_{\ 0}$ and pressure $p_F = -\frac{2}{3}E_i^{\ i}$, implying that the whole effective dark energy density and pressure consist of two parts each:

$$\rho_{\Lambda\text{eff}}(t) = \rho^i_\Lambda + \rho_F(t), \qquad p_{\Lambda\text{eff}}(t) = -\rho^i_\Lambda + p_F(t). \tag{2.5}$$

As announced, they follow the structure of the ΛXCDM model [13], as both are the sum of a cosmological term energy density (resp. pressure) and an extra contribution whose structure derives from the presence of new terms in the effective action. The local energy density ρ_F constitutes the "induced DE density" for this model. It is indeed induced by the new term of the modified gravity action (2.1). However, the only measurable DE density in our model is the effective vacuum energy $\rho_{\Lambda\text{eff}}$ in (2.5), i.e. the sum of the initial (arbitrarily large) vacuum energy density ρ^i_Λ and the induced DE density ρ_F. None of the latter, though, is individually measurable. Let us note that the induced DE density is covariantly self-conserved, i.e. independently of matter (which is also conserved). Indeed, the Bianchi identity on the FLRW background leads to the local covariant conservation laws

$$\dot{\rho_n} + 3H(\rho_n + p_n) = 0\,, \tag{2.6}$$

which are valid for all the individual components (n = radiation, matter and vacuum) with energy density ρ_n and pressure p_n. This leads immediately to the usual expressions $\rho_m = \rho_m^0 a^{-3}$ and $\rho_r = \rho_r^0 a^{-4}$ for cold matter and radiation respectively. As for the effective vacuum energy density $\rho_{\Lambda\text{eff}}$, since ρ_Λ^i is a true CC term and satisfies $p_\Lambda^i = -\rho_\Lambda^i$, it follows that the F-term density is self-conserved:

$$\dot{\rho}_F + 3H(\rho_F + p_F) = \dot{\rho}_F + 3H\,[1+\omega_F(t)]\,\rho_F = 0\,, \tag{2.7}$$

where $\omega_F = \omega_F(t)$ is the corresponding (non-trivial) effective equation of state (EoS) of the F-term. We shall come back to it in more detail in Sect. 5.

The cosmological evolution is therefore completely determined by the generalized Friedmann equation of our model,

$$\frac{3H^2}{8\pi G} = \rho_m + \rho_{\Lambda\text{eff}} = \rho_m + \rho_\Lambda^i + \rho_F, \tag{2.8}$$

where $\rho_m \propto a^{-3}$ denotes the energy density of the (self-conserved) matter, which is mostly dust-like matter for the purpose of this paper (as we focus mainly on the matter dominated and DE epochs).

Next, we consider the CC relaxation mechanism from Refs. [4, 11], in which F in the action (2.1) is picked within the class of functions $F_m^n = F_m^n(R,\mathcal{G})$ of the form

$$F_m^n = \beta\frac{R^n}{(B(R,\mathcal{G}))^m} \equiv \beta\frac{R^n}{\left[\frac{2}{3}R^2 + \frac{1}{2}\mathcal{G} + (y\,R)^3\right]^m}\,. \tag{2.9}$$

Here β and y are two parameters of the model, and $n \geq 0$ and $m > 0$ (usually taken to be integers) are two numbers characterizing a large class of functions that can realize the relaxation mechanism. To understand how the mechanism works in modified gravity, let us express the denominator of (2.9) in terms of H and q,

$$B(H,q) = 24H^4(q-\frac{1}{2})(q-2) + \left[6\,y\,H^2(1-q)\right]^3. \tag{2.10}$$

Taking into account that each derivative of F in Eqs. (2.3) and (2.4) increases the power of the denominator function B, it is easy to see that the induced energy density ρ_F and pressure p_F have at least one positive power of B in their denominators. Schematically, one can show that it takes on the form

$$\rho_F(t) = \frac{f_1(t)}{B^m} + \frac{f_2(t)}{B^{m+1}} + \frac{f_3(t)}{B^{m+2}}\,, \tag{2.11}$$

with f_i being time-dependent functions not containing the factor B. Notice that we need $n < 2m$ in order that ρ_F can increase with the expansion, i.e. when H is decreasing. In this case, the gravity modification F in the action (2.1) will be able to compensate the large initial vacuum energy density ρ_Λ^i in the field equations (2.2), whatever it be its value and size, by $\rho_F = 2\,E_0^0$ becoming large in a dynamical manner. It means that ρ_F can take the necessary value to compensate for the big initial ρ_Λ^i, this being achieved automatically because B becomes small during the radiation dominated regime ($q \to 1$), then also in

the matter dominated era ($q \to \frac{1}{2}$), and finally again in the current universe and in the asymptotic future, where H becomes very tiny.

A few additional observations are in order. The fact that we search our relaxation functionals among those of the form $F(R, \mathcal{G})$ is because they are better behaved. Indeed, let us recall that general modified gravity models of the form $F(R, S, T)$, with $R = g^{ab}R_{ab}$, $S = R_{ab}R^{ab}$ and $T = R_{abcd}R^{abcd}$, are generally problematic as far as ghosts and other instabilities are concerned. This is because these theories introduce new degrees of freedom, which potentially lead to instabilities not present in general relativity (GR). They may e.g. suffer from the Ostrogradski instability, i.e. they may involve vacuum states of negative energy. In general they contain gravitational ghosts and can lead to various types of singularities. These issues are discussed e.g. in [21] and are reviewed in [22]. Fortunately, some of these problems can be avoided by specializing to $F(R, \mathcal{G})$ functionals involving only the Ricci scalar and the Gauß-Bonnet invariant [23]. The reason is that all functionals of the form $F(R, T-4S)$ are ghost free [24], a property which is shared by our functionals because $\mathcal{G} = R^2 - 4S + T$.

Finally, the $F(R, \mathcal{G})$ theories are thought to have a more reasonable behavior in the solar system limit [24, 25]. A detailed study of the astrophysical consequences of our model was presented in [12]. It shows that a huge cosmological constant can also be relaxed in astrophysical systems such as the solar system and the galactic domain. These studies were performed by solving the field equations in the Schwarzschild-de Sitter metric in the presence of an additional $1/R$ term. The latter operates the relaxation of the huge CC at astrophysical scales in a similar way as the $\sim 1/B$ term in equation (2.9) does it in the cosmological domain. One can show that none of these terms has any significant influence in the region of dominance of the other. Therefore a huge CC can be reduced both in the local astrophysical scales and in the cosmological one in the large. The solution in the Schwarzschild-de Sitter metric merges asymptotically with the cosmological solution, where we recover the original framework presented in [4]. Furthermore, it was shown in [12] that there are no additional (long range) macroscopic forces that could correct in a measurable way the standard Newton's law. This is a consequence of the dynamical relaxation mechanism and is in contrast to ordinary modified gravity models. The upshot is that the implementation of the relaxation mechanism should not be in conflict with local gravitational experiments. At the same time, we expect small deviations from GR only at scales of a few hundred kpc at least, which is in accordance with other authors [26]. As this scale is much larger than the scale where star systems can be tested at the level of GR, the physics of these local astrophysical objects should not be affected.

2.1 Physical scales for the relaxation mechanism

Remarkably, in order to insure that $|\rho_\Lambda^i + \rho_F| \ll |\rho_\Lambda^i|$ holds at all times, we need not fine tune the value of any parameter of the model. It is only necessary that the parameter β in the class of invariants (2.9) has the right order of magnitude and sign. This requirement has nothing to do with fine tuning, as fine tuning means to adjust by hand the value of the parameter β to some absurd precision such that both (big) terms ρ_Λ^i and ρ_F almost cancel each other in (2.5). This is not necessary at all for our mechanism to work because it is

dynamical, meaning that it is the evolution itself of the universe through the generalized Friedmann equation (2.8) what drives the F-term density ρ_F towards almost canceling the huge initial ρ_Λ^i in each relevant stage of the cosmic evolution (i.e. in the radiation dominated, matter dominated and dark energy dominated epochs). In this way we can achieve the natural relation

$$\frac{\rho_{\Lambda\text{eff}}}{\rho_\Lambda^i} = \frac{\rho_\Lambda^i + \rho_F(H_*)}{\rho_\Lambda^i} = \frac{\rho_c^0 - \rho_m^0}{\rho_\Lambda^i} = \mathcal{O}\left(\frac{\rho_c^0}{\rho_\Lambda^i}\right) \ll 1, \tag{2.12}$$

for some value of H_* sufficiently close to H_0. The smallness of the observed $\rho_{\Lambda\text{eff}}$ as compared to the huge initial ρ_Λ^i thus follows from the right-hand side of (2.12) being suppressed by the ratio of the present critical density $\rho_c^0 = 3H_0^2/(8\pi G)$ as compared to its initial value in the early universe, which was of course of order ρ_Λ^i. By working out the explicit structure of (2.11) from (2.3), and using the fact that $\dot{H} = -(q+1)H^2$, we can easily convince ourselves that all terms end up roughly in the form $\rho_F(H) \sim \beta\, H^{2n-4m}$. Although we are omitting here other terms, we adopt provisionally that expression for the sake of simplicity (see the next section for more details). Within this simplified setup, it follows that the value of H_* that solves equation (2.12) – which, as we said, should be close enough to the current value of H – is approximately given by

$$H_*^2 \simeq \left|\frac{\beta}{\rho_\Lambda^i}\right|^{1/(2m-n)}. \tag{2.13}$$

We see that for $n < 2m$ this mechanism provides also a natural explanation for the current value of H being so small: the reason simply being that ρ_Λ^i is very large! Moreover, we can make H_* of order of the measured H_0 provided β has the right order of magnitude (without operating any fine tuning). Notice that since the power mass dimension of β for the F_m^n models is

$$|\beta| = \mathcal{M}^{4-2n+4m}, \tag{2.14}$$

and $\rho_\Lambda^i \sim M_X^4$, it follows that $H_* \equiv H_0$ is related to $\mathcal{M}$ through

$$H_0 \simeq \mathcal{M}\left(\frac{\mathcal{M}}{M_X}\right)^{2/(2m-n)}. \tag{2.15}$$

For the simplest F_1^0 model this implies $\mathcal{M} \sim \sqrt{M_X H_0}$, and therefore if M_X is near M_P we obtain $\mathcal{M}$ around the characteristic meV scale associated to the current CC density: $m_\Lambda \equiv \left(\rho_\Lambda^0\right)^{1/4} \sim 10^{-3}$ eV. On the other hand, for the models F_1^1 and F_2^3 we find in both cases $\mathcal{M} \sim \left(M_X^2\, H_0\right)^{1/3}$, which implies $\mathcal{M} \sim 0.1 - 100\,\text{MeV}$ for M_X in the ballpark of the GUT scale ($\sim 10^{16}$ GeV) up to the Planck mass $M_P \sim 10^{19}$ GeV. This is certainly a possible mass scale in the SM of Particle Physics.

Notice that equations (2.13) and (2.15) have been derived under the assumption $n \neq 2m$. Therefore, the conclusion that the current value of H is small because ρ_Λ^i is large cannot be inferred from equation (2.13) if $n = 2m$. Still, we shall see in the next next section that a more accurate treatment of the $n = 2m$ models leads once more to the

conclusion that the current H is small. What else can be learnt from equation (2.15)? Notice that it can be rewritten as

$$2m - n \simeq 2\,\frac{\ln\left(M_X/\mathcal{M}\right)}{\ln\left(\mathcal{M}/H_0\right)} \simeq \frac{2(s-r)}{r+42}\,, \tag{2.16}$$

with $M_X \equiv 10^s$ GeV, $\mathcal{M} \equiv 10^r$ GeV and $H_0 \sim 10^{-42}$ GeV (for some integers r and s). Now, being $M_X \leqslant M_P \sim 10^{19}$ GeV the GUT scale, we must have $r \leqslant s \leqslant 19$. For $r \geqslant 0$, it follows from (2.16) that $0 \leqslant 2m - n \lesssim 1$. But let us keep in mind that we could have $r < 0$. Since, however, the scale $\mathcal{M}$ should not be too tiny [4], it is natural to assume that it is not much smaller than the typical meV scale associated to the CC density, i.e. we must have $\mathcal{M} \gtrsim m_\Lambda \sim$ meV$= 10^{-12}$ GeV, which enforces $r \gtrsim -12$. Thus e.g. in the extreme case $s = 19$ and $r = -12$, we have $2m - n \lesssim 3$. The upshot of this (order of magnitude) consideration is that, with r bounded in the approximate interval $-12 \lesssim r \leqslant s$, we should expect in general that the following combined "natural relaxation condition" is fulfilled:

$$0 \leqslant 2m - n < \mathcal{O}(1)\,, \tag{2.17}$$

in which both naturalness of the mass scales and relaxation of the vacuum energy are insured. In other words, the above argument suggests that if n and m are taken as integers, we cannot assume large values for them (unless $n = 2m$) because the relation (2.17) could not be fulfilled. This is of course a welcome feature because it suggests that only the canonical cases are natural candidates, namely $(n, m) = (0, 1), (1, 1), (2, 1), (3, 2)$ and $(2, 2)$ at most – the last case of this series being the one which approaches the most to the upper bound imposed by the relation (2.17), but still the difference is of $\mathcal{O}(1)$. The next model in the list, $(n, m) = (2, 3)$, tenses up a bit too much perhaps that bound, so for definiteness we stop the number of candidate models to the first five in the list. Of course the models with $n = 2m$ for arbitrary n would do, but again it is natural to focus on only the canonical representative $(n, m) = (2, 1)$ of this class. In general the class $n = 2m$ is special because, as we can see from equation (2.16), it requires $\mathcal{M} = M_X$. Therefore, if $M_X \sim 10^{16}$ GeV is a typical large GUT scale, then $\mathcal{M}$ must coincide with it. We may think of the $n = 2m$ models as the class of "no-scale" relaxation models inasmuch as they do not introduce any other new scale beyond the one associated to the initial vacuum energy itself, $M_X = \left(\rho_\Lambda^i\right)^{1/4}$. Also interesting about the "no-scale models" is to note that if there is no GUT scale above the SM of Particle Physics, i.e. if M_X turns out to be just the electroweak scale $M_W = \mathcal{O}(100)$ GeV, then the relaxation mass parameter $\mathcal{M}$ will naturally take on the order of magnitude value M_W, characteristic of the electroweak gauge boson masses, for all the relaxation models $n = 2m$. Remarkably, it is the only situation where we can accommodate the electroweak scale M_W in the relaxation mechanism.

To summarize, even though we have in principle five canonical candidate models satisfying the natural relaxation condition (2.17), on the whole they involve only two new

[4] If $\mathcal{M}$ could be very small, we would stumble upon the same tiny mass problem that afflicts e.g. all quintessence-like models [5], where mass scales as small as $H_0 \sim 10^{-33}$ eV are a common place. This is one, but certainly not the only one, of the most serious drawbacks of these models, another one being of course the need of extreme fine-tuning. In our case, however, we aim precisely at avoiding both of these severe problems.

physical scales for the dynamical adjustment of the cosmological constant, to wit: the two models $F_1^0 \sim F_2^2$ are both linked to the same mass scale $\mathcal{M}_1$ close to the one inherent to the current CC density, $\mathcal{M}_1 \sim m_\Lambda \sim 10^{-3}$ eV, whereas the two models $F_1^1 \sim F_2^3$ are both associated to the scale $\mathcal{M}_2 \sim 0.1 - 100$ MeV, which is a typical Particle Physics scale within the SM of electroweak and strong interactions. Thus both scales quite natural ones. On the other hand the fifth model F_1^2 (and, for that matter, the entire F_m^{2m} class) is a "no-scale" model which is able to operate the relaxation mechanism by using the very same scale as the one associated to $\rho_\Lambda^i \sim M_X^4$, irrespective of M_X being a huge GUT scale or just the electroweak scale of the SM.

As for the dimensional parameter y in (2.10), let us note that it is basically irrelevant for the present discussion. In Ref. [4], this parameter played a role only in the radiation dominated epoch and did not suffer any fine tuning either; it just had to take a value within order of magnitude. In practice the whole structure $(y\,R)^3$ of the last term in equation (2.10) was motivated by considerations related to getting a smooth transition from the radiation to the matter dominated epochs. Since, however, we are now comparing the class of models (2.9) with the observations, all the relevant data to which we can have some access belong to the matter dominated epoch until the present time (apart from a correction from the radiation term in the case of the CMB data, which has been duly taken into account, see Sect. 3). We have indeed confirmed numerically that the last term on the *r.h.s.* of equation (2.10) is unimportant for the present analysis.

2.2 A closer look to the general structure of the induced DE density ρ_F

After we have presented the simplest version of the relaxation mechanism, it seems appropriate to discuss a bit further the general behavior of the F-density ρ_F in order to better understand the relaxation mechanism in the different cases. Following the considerations exposed at the end of the last section, hereafter we will set $y = 0$ in equation (2.10). We start by considering the the general structure of the F-density $\rho_F = 2E_0^0$ for an arbitrary F_m^n model, which as we know can be cast as in equation (2.11). However, by dimensional analysis and the explicit structure of (2.3) and (2.10), it is not difficult to convince oneself that it can eventually be brought into the more specific form:

$$\rho_F(H, q, \dot{q}/H) = \frac{\beta}{H^{4m-2n}} \left[f(q) + g(q)\,\frac{\dot{q}}{H} \right] . \tag{2.18}$$

Here $f(q)$ and $g(q)$ are functions of q which are different for different F_m^n models, but in all cases they are rational functions of q with a (multiple) pole at $q = 1/2$, specifically $f(q) \propto 1/b^k$, $g(q) \propto 1/b^{k+1}$, where for convenience we have defined the following expression that appears in the calculation:

$$b := 2(q - \frac{1}{2})(q - 2)\,. \tag{2.19}$$

For specific realizations of equation (2.18), see Appendix A. Let us note that because of the pole at $q = 1/2$ all these models have an unstable fixed point in the matter dominated epoch, which is responsible for the universe to approach $q \to 1/2$ for a long while during

that epoch and at the same time enhances dynamically the value of ρ_F. As a result the huge value of the vacuum energy can be relaxed from ρ_Λ^i to the effective tiny $|\rho_{\Lambda\rm eff}| \ll |\rho_\Lambda^i|$, which can be identified with $\rho_{\Lambda\rm eff} = \rho_\Lambda^0$ at the present time. When that pole is left behind during the cosmic evolution, the relaxation mechanism can still work effectively provided H tends to a very small value in the present universe. Notice that there are two terms in equation (2.18) that cooperate to fulfill this end: one of them is the overall $\sim 1/H^{4m-2n}$ factor, which contributes to the relaxation mechanism provided n is strictly smaller than $2m$, as indeed required by the relation (2.17); and the other is the term $\dot{q}/H$ in the parentheses. For all the models such that $n < 2m$, the first term suffices and in this way we recover the result (2.13) which we had sketched in the simplified exposition of Sect. 2.1.

However, if $n = 2m$ the simplified argument of Sect. 2.1 cannot be applied. The class of these "no-scale" functionals is of the form $F_m^{2m} \sim M_X^4 R^{2m}/B^m$, where the relevant parameter is M_X, the same one as that associated to $\rho_\Lambda^i \sim M_X^4$. As previously noticed, this is the only case where the scale $\mathcal{M}$ defined in (2.14) could be identical to the initial vacuum energy scale $M_X \equiv \left(\rho_\Lambda^i\right)^{1/4} \geq 10^{16}$ GeV of the GUT at the early universe, which is a very interesting possibility in that here the mechanism for canceling the large vacuum energy density of the early universe would be naturally dealt with by the very same scale pertaining to the GUT transition at that time. For the $n = 2m$ models, the factor $\dot{q}/H$ inside the parenthesis in equation (2.18) takes its turn in the relaxation mechanism. Noting that now equation (2.18) simplifies to

$$\rho_F(q, \dot{q}/H) = \beta \left[f(q) + g(q)\, \frac{\dot{q}}{H} \right] \qquad (n = 2m)\,, \tag{2.20}$$

it follows that the relaxation condition (2.12) for the present universe enforces H_* to take the value

$$H_* = \left| \frac{\beta\, g(q)\, \dot{q}}{\beta\, f(q) + \rho_\Lambda^i} \right| \sim \left| \frac{\beta}{\rho_\Lambda^i}\, g(q)\, \dot{q} \right| \sim |g(q)\dot{q}| \sim |\dot{q}|\ . \tag{2.21}$$

In this equation we have used the fact that, for the $n = 2m$ models, we have $\beta = M_X^4$, which is of the same order of magnitude as $\rho_\Lambda^i \sim M_X^4$ and therefore the two factors cancel out approximately. Finally, $g(q)$ is a dimensionless function, basically a number which can be taken of order 1 in this kind of consideration. Therefore, we conclude that the predicted value of the current expansion rate for these models is $H_* \sim |\dot{q}|$, and therefore it can naturally be of order H_0. So, again, the relaxation mechanism works and requires a very small value for the present Hubble rate.

3. Likelihood analysis from CMB, SNIa, BAO and $H(z)$ data

In the following we briefly present some details of the statistical method and on the observational samples and data statistical analysis that will be adopted to constrain the relaxation models presented in the previous section. First of all, we use the *Constitution* set of 397 type Ia supernovae of Hicken et al. [27]. In order to avoid possible problems related with the local bulk flow, we use a subsample of 366 SNIa, excluding those with $z < 0.02$. The

corresponding $\chi^2_{\rm SNIa}$ function, to be minimized, is:

$$\chi^2_{\rm SNIa}(\mathbf{p}) = \sum_{i=1}^{366} \left[\frac{\mu_{\rm th}(a_i, \mathbf{p}) - \mu_{\rm obs}(a_i)}{\sigma_i} \right]^2 , \tag{3.1}$$

where $a_i = (1+z_i)^{-1}$ is the observed scale factor of the Universe for each data point and z_i the corresponding (measured) redshift. The fitted quantity μ is the distance modulus, defined as $\mu = m - M = 5 \log d_L + 25$, in which $d_L(a, \mathbf{p})$ is the luminosity distance:

$$d_L(a, \mathbf{p}) = \frac{c}{a} \int_a^1 \frac{{\rm d}a'}{a'^2 H(a')} = c(1+z) \int_0^z \frac{{\rm d}z'}{H(z')} , \tag{3.2}$$

with c the speed of light and $\mathbf{p} = (\Omega_m, q_0, \dot{q}_0/H_0)$ a vector containing the cosmological parameters of our model that we wish to fit for. In equation (3.1), the theoretically calculated distance modulus $\mu_{\rm th}$ for each point follows from using (3.2), in which the Hubble function is given by the generalized Friedmann's equation (2.8). Finally, $\mu_{\rm obs}(a_i)$ and σ_i stand for the measured distance modulus and the corresponding 1σ uncertainty for each SNIa data point, respectively. The previous formula (3.2) for the luminosity distance applies only for spatially flat universes, which we are assuming throughout.

On the other hand, a very interesting geometrical probe of dark energy is provided by the measures of $H(z)$ [20] from the differential ages of passively evolving galaxies [hereafter $H(z)$ data] [5]. This sample of galaxies contains 11 entries spanning a redshift range of $0 \leq z < 2$, and the corresponding $\chi^2_{\rm H}$ function can be written as:

$$\chi^2_{\rm H} = \sum_{i=1}^{11} \left[\frac{H_{\rm th}(z_i, \mathbf{p}) - H_{\rm obs}(z_i)}{\sigma_i} \right]^2 . \tag{3.3}$$

Note that the latter set of data became recently interesting and competitive for constraining dark energy, see e.g. [28].

In addition to the SNIa and $H(z)$ data, we also consider the BAO scale produced in the last scattering surface by the competition between the pressure of the coupled baryon-photon fluid and gravity. The resulting acoustic waves leave (in the course of the evolution) an overdensity signature at certain length scales of the matter distribution. Evidence of this excess has been found in the clustering properties of the SDSS galaxies (see [19], [29]) and it provides a "standard ruler" that we can employ to constrain dark energy models. In this work we use the measurement derived by Eisenstein et al. [19]. In particular, we utilize the following estimator

$$A(\mathbf{p}) == \frac{\sqrt{\Omega_m^0}}{[z_s^2 E(z_s)]^{1/3}} \left[\int_0^{z_s} \frac{dz}{E(z)} \right]^{2/3} , \tag{3.4}$$

with $E(z) = H(z)/H_0$ the normalized Hubble rate. The previous estimator is measured from the SDSS data to be $A = 0.469 \pm 0.017$, where $z_s = 0.35$ [or $a_s = (1+z_s)^{-1} \simeq 0.75$]. Therefore, the corresponding $\chi^2_{\rm BAO}$ function can be written as:

$$\chi^2_{\rm BAO}(\mathbf{p}) = \frac{[A(\mathbf{p}) - 0.469]^2}{0.017^2} . \tag{3.5}$$

[5] For the current value of the Hubble constant, we use $H_0 \equiv 100\, h = 73\, {\rm km/s/Mpc}$ [28].

Finally, a very accurate and deep geometrical probe of dark energy is the angular scale of the sound horizon at the last scattering surface, as encoded in the location l_1^{TT} of the first peak of the Cosmic Microwave Background (CMB) temperature perturbation spectrum. This probe is described by the CMB shift parameter [30, 31], defined as:

$$R = \sqrt{\Omega_m^0} \int_{a_{ls}}^{1} \frac{da}{a^2 E(a)} = \sqrt{\Omega_m^0} \int_0^{z_{ls}} \frac{dz}{E(z)} \,. \tag{3.6}$$

The measured shift parameter according to the WMAP 7-years data [1] is $R = 1.726 \pm 0.018$ at the redshift of the last scattering surface: $z_{ls} = 1091.36$ [or $a_{ls} = (1 + z_{ls})^{-1} \simeq 9.154 \times 10^{-4}$]. In this case, the $\chi^2_{\rm cmb}$ function is given by:

$$\chi^2_{\rm cmb}(\mathbf{p}) = \frac{[R(\mathbf{p}) - 1.726]^2}{0.018^2} \,. \tag{3.7}$$

Let us note that when dealing with the CMB shift parameter we have to include both the matter and radiation terms in the total normalized matter density entering the $E(z)$ function in (3.6):

$$\Omega_m(z) = \Omega_m^0 \, (1+z)^3 + \Omega_R^0 \, (1+z)^4 \,. \tag{3.8}$$

Indeed, we have $\Omega_R^0 = (1 + 0.227 N_\nu) \, \Omega_\gamma^0$, with N_ν the number of neutrino species and $\Omega_\gamma^0 \, h^2 \simeq 2.47 \times 10^{-5}$. Therefore, at $z_{ls} = 1091.36$ and for three light neutrino species the radiation contribution amounts to some 24% of the total energy density associated to matter. For a detailed discussion of the shift parameter as a cosmological probe, see e.g. [32].

In order to place tighter constraints on the corresponding parameter space of our model, the probes described above must be combined through a joint likelihood analysis[6], given by the product of the individual likelihoods according to:

$$\mathcal{L}_{\rm tot}(\mathbf{p}) = \mathcal{L}_{\rm SNIa} \times \mathcal{L}_{\rm H} \times \mathcal{L}_{\rm BAO} \times \mathcal{L}_{\rm cmb} \,, \tag{3.9}$$

which translates in an addition for the joint χ^2 function:

$$\chi^2_{\rm tot}(\mathbf{p}) = \chi^2_{\rm SNIa} + \chi^2_{\rm H} + \chi^2_{\rm BAO} + \chi^2_{\rm cmb} \,. \tag{3.10}$$

In order to proceed with our χ^2 minimization procedure, we would like to reduce as much as possible the free parameter space by imposing a prior, specifically we fix the value of the current mass parameter $\Omega_m^0 = \rho_m^0/\rho_c^0$. In principle, Ω_m^0 is constrained by the maximum likelihood fit to the WMAP and SNIa data in the context of the concordance Λ cosmology, but in the spirit of the current work, we want to use measures which are completely independent of the dark energy component. An estimate of Ω_m^0 without conventional priors is not an easy task in observational cosmology. However, various authors, using mainly large scale structure studies, have attempted to put constraints to the Ω_m^0 parameter. In a

[6]Likelihoods are normalized to their maximum values. In the present analysis we always report 2σ uncertainties on the fitted parameters. Note also that the total number of data points used here is $N_{\rm tot} = 379$, while the associated degrees of freedom is: $dof = N_{\rm tot} - n_{\rm fit}$, where $n_{\rm fit}$ is the model-dependent number of fitted parameters.

rather old paper Plionis et al. [33] using the motion of the Local Group with respect to the cosmic microwave background found $\Omega_m^0 \simeq 0.30$. From the analysis of the power spectrum, Sanchez et al. [34] obtain a value $\Omega_m^0 \simeq 0.24$. Moreover, [35] and [36] analyze the peculiar velocity field in the local Universe and obtain the values $\Omega_m^0 \simeq 0.30$ and $\simeq 0.22$ respectively. In addition, the authors of Ref. [37], based on the cluster mass-to-light ratio, claim that Ω_m^0 lies in the interval $0.15 - 0.26$ (see also [38] for a review). Therefore, there are strong independent indications for $0.2 \lesssim \Omega_m^0 \lesssim 0.3$, and in order to compare our results with those of the flat ΛCDM we will restrict our present analysis to the choice $\Omega_m^0 = 0.27$. If we fix the value of Ω_m^0, then the corresponding vector $\mathbf{p}$ contains only two free parameters namely, $(q_0, \dot{q}_0/H_0)$. Note that we sample $q_0 \in [-1.24, 0.1]$ and $\dot{q}_0/H_0 \in [-5, 0.2]$ in steps of 0.001.

4. Identifying the best relaxation F_m^n models from observation

In order to select the optimal relaxation models F_m^n, defined in Eq. (2.9), from the phenomenological point of view, we are going to perform a likelihood analysis along the lines described in the previous section. Specifically, we will use a two-parameter fit of our models. Namely, for any given F_m^n model with fixed m and n, we have to look for the best fit values for q_0 and $\dot{q}_0/H_0$.

4.1 Numerical solution of the F_m^n models

Remember that the parameters q_0 and $\dot{q}_0$ are necessary in order to establish the initial conditions for solving the generalized Friedmann equation (2.8), in which $\rho_{\Lambda\text{eff}}$ is a complicated function of the form $\rho_{\Lambda\text{eff}}(H, q, \dot{q}/H) = \rho_\Lambda^i + \rho_F(H, q, \dot{q}/H)$. Using $\dot{H} = -H^2(q+1)$ one can see that $\rho_{\Lambda\text{eff}} = \rho_{\Lambda\text{eff}}(H, \dot{H}, \ddot{H})$ and hence the generalized Friedmann equation, despite its innocent appearance, becomes a third order differential equation in the scale factor [7] $a = a(t)$. Therefore, since the current H_0 is known, we need to input q_0 and $\dot{q}_0$ for any given relaxation model F_m^n. Notice also that the initial values of q_0 and $\dot{q}_0$ must be consistent with the current value of Ω_Λ^0, which in our case is identified with

$$\Omega_{\Lambda\text{eff}}^0 = \frac{\rho_\Lambda^i + \rho_F(H_0, q_0, \dot{q}_0)/H_0}{\rho_c^0} = 1 - \Omega_m^0\,, \tag{4.1}$$

for flat space cosmology. For the reasons indicated in Sect. 2.1, we will limit ourselves to analyze the five canonical models F_1^0, F_1^1, F_2^3, F_1^2 and F_2^2 using the combined likelihood method described in the previous section. We present a sample of the likelihood contours in the $(q_0, \dot{q}_0/H_0)$ plane for the individual sets of data on SNIa, CMB shift parameter, BAO and $H(z)$ in Figs. 1-3, whereas in Fig. 4 we display the combined likelihood contours for all the five models. A numerical summary of the statistical analysis for these models is shown in Table 1. In the next section, we provide more details of this analysis and discuss the obtained results.

[7] Although equation (2.4) indicates that, in principle, the field equations are of fourth order, the self-conservation of ρ_F, see (2.7) (and hence also of the effective vacuum energy $\rho_{\Lambda\text{eff}}$), enables us to reduce the order of the field equations by one unit.

Table 1: Results of the overall likelihood function analysis, equation (3.10). The 1st column indicates the various F_m^n models. The ΛCDM model is included in the first row for comparison, although in this case we present the theoretical prediction based on equations (4.2) and (4.3). The 2nd, 3rd and 4th columns show the best fit parameters and the reduced $\chi^2_{\rm tot}$. We use the prior $\Omega_m^0 = 0.27$, flat space cosmology and the (arbitrarily chosen) initial vacuum energy such that $\rho_\Lambda^i/\rho_c^0 = -10^{60}$ for all the models. In the final column one can find various line types appearing in Fig. 4 where all models are plotted together.

Model	q_0	$\dot{q}_0/H_0$	$\chi^2_{\rm tot}/377$	Symbols
ΛCDM	-0.595	-0.887		
F_1^0	-0.506 ± 0.04	-0.43 ± 0.03	1.188	red dashed
F_1^1	-0.500 ± 0.03	-0.36 ± 0.07	1.187	magenta long-dashed
F_2^3	-0.551 ± 0.04	-0.63 ± 0.07	1.186	black solid
F_1^2	-0.678 ± 0.04	-2.27 ± 0.34	1.188	green dotted
F_2^2	-0.520 ± 0.06	-0.480 ± 0.05	1.187	black dotted area

4.2 The Statistical Results

In the upper left panel of Fig. 1 we present the results of our analysis for the F_1^0 model in the $(q_0, \dot{q}_0/H_0)$ plane. The individual contours for each observable are plotted only for the 1σ and 2σ confidence levels in order to avoid confusion. In particular, the SNIa-based results indicated by thin solid lines, the $H(z)$ results by thick dot-dashed lines, the BAO results by dotted lines and those based on the CMB shift parameter by thin dashed lines. The remaining panels show the statistical results for SNIa/BAO, SNIa/$H(z)$ and SNIa/CMB. Using the SNIa/BAO data alone it is evident that the $\dot{q}_0/H_0$ parameter is unconstrained within 2σ errors. However, within 1σ errors we can put some constraints (the best fit values are $q_0 \simeq -0.56$ and $\dot{q}_0/H_0 \simeq -0.64$). On the other hand, utilizing the SNIa/$H(z)$ data the best fit parameters are partially constrained within 2σ: $q_0 \simeq -0.516$ and $\dot{q}_0/H_0 \simeq -0.47$. As can be seen in the lower right panel of Fig. 1, the above degeneracy is broken when using the SNIa/CMB data and practically the best fit parameters coincide with those of joint likelihood analysis, involving all the cosmological data. Indeed, for the F_1^0 model we find that the overall likelihood function peaks at $q_0 = -0.506 \pm 0.04$ and $\dot{q}_0/H_0 \simeq -0.43 \pm 0.03$ with $\chi^2_{\rm tot} \simeq 447.83$ for 377 degrees of freedom.

In the case of the "no-scale" F_1^2 model we find that only the combined SNIa/CMB data can put constraints on the free parameters (see Fig. 2), while the overall likelihood analysis provides $q_0 = -0.678 \pm 0.04$ and $\dot{q}_0/H_0 = -2.27 \pm 0.34$ with $\chi^2_{\rm tot} \simeq 447.83$ for 377 degrees of freedom. Concerning the F_1^1 model (see Fig. 3) we find that the corresponding statistical results are in a very good agreement to those of the F_1^0 model. Indeed, the SNIa/BAO data put some constraints within 1σ errors, $q_0 \simeq -0.56$ and $\dot{q}_0/H_0 \simeq -0.66$ while using the SNIa/$H(z)$ data we find $q_0 \simeq -0.530$ and $\dot{q}_0/H_0 \simeq -0.441$. Again we observe that the joint likelihood function (mainly due to SNIa/CMB) peaks at $q_0 = -0.50 \pm 0.03$ and $\dot{q}_0/H_0 \simeq -0.36 \pm 0.07$ with $\chi^2_{\rm tot} \simeq 447.5$ for 377 degrees of freedom. As for the F_2^3 model, again we find that the comparison between SNIa/BAO does not place constraints on the free

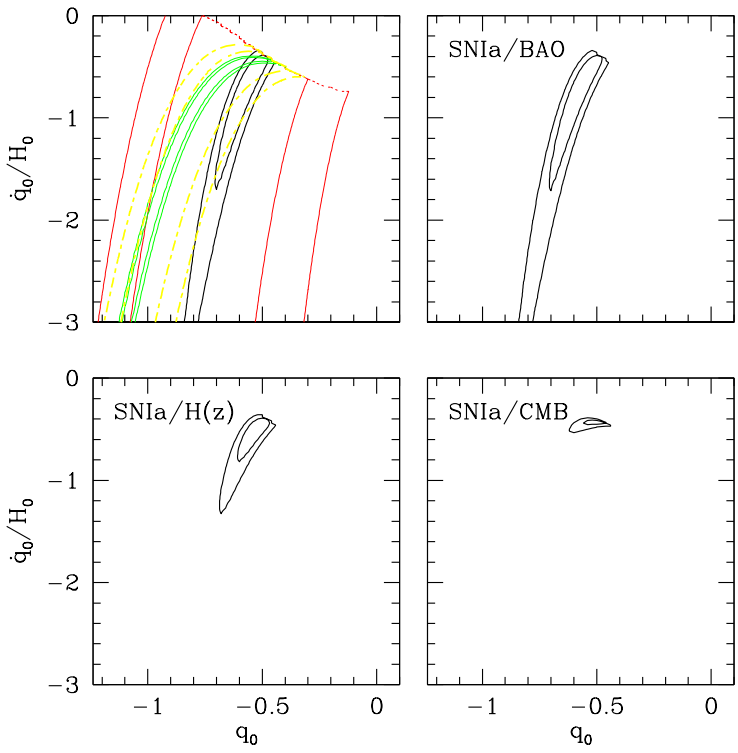

Figure 1: F_1^0 *model:* Likelihood contours in the $(q_0, \dot{q}_0/H_0)$ plane. The contours are plotted where $-2\ln(\mathcal{L}/\mathcal{L}_{\max})$ is equal to 2.32 and 6.16, corresponding to 1σ and 2σ confidence level. We do not plot the 3σ contour in order to avoid confusion. In the upper left panel we present the likelihood contours that correspond to the SNIa (solid lines), $H(z)$ (yellow thick dot-dashed lines), CMB/shift parameter (green dashed lines) and BAOs observational data (red dotted lines). The remaining panels show the statistical results for different pairs.

parameters while the SNIa/$H(z)$ data put some constrains (even within 1σ): $q_0 \simeq -0.547$ and $\dot{q}_0/H_0 \simeq -0.63$. As before, the free parameters of the model are tightly constrained by the SNIa/CMB data. The joint likelihood function peaks at $q_0 = -0.551 \pm 0.04$ and $\dot{q}_0/H_0 = -0.63 \pm 0.07$ with $\chi^2_{\rm tot} \simeq 447.12$ for 377 degrees of freedom. To this end for the F_2^2 model we find that the SNIa/$H(z)$ comparison implies $q_0 \simeq -0.540$ and $\dot{q}_0/H_0 \simeq -0.58$ while using the joint likelihood analysis we find $q_0 = -0.52 \pm 0.06$ and $\dot{q}_0/H_0 = -0.48 \pm 0.05$ with $\chi^2_{\rm tot} \simeq 447.53$ for 377 degrees of freedom. Although we do not present individual likelihood contours for the F_2^3 and F_2^2 models, we can see their overall likelihood contours in Fig. 4, together with those of the other models.

The summarized analysis of all the five canonical relaxation models is presented in Table 1 and in Fig. 4. In this combined figure we plot the 1σ, 2σ, and also the 3σ, overall likelihood contours for the five the models under consideration. In it we can see a compact presentation of all our statistical results including their comparison with the corresponding values of $(q_{0\Lambda}, \dot{q}_{0\Lambda}/H_0)$ for the concordance or traditional ΛCDM model. Let us note that

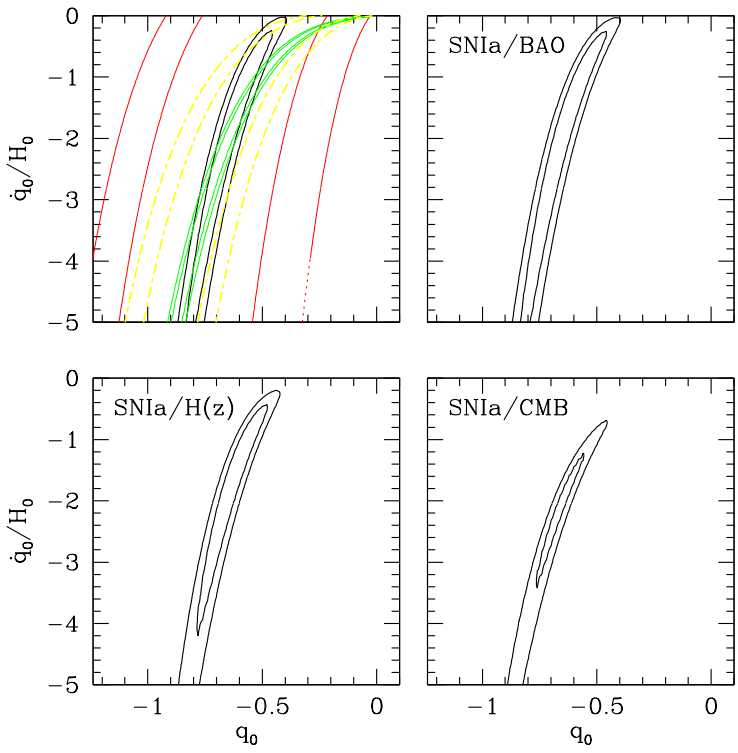

Figure 2: F_1^2 *model* (or *"no-scale"* relaxation model): The Likelihood contours in the $(q_0, \dot{q}_0/H_0)$ plane. The different observational data are represented by different line types (see caption of Fig. 1 for definitions).

the $(q_\Lambda(z), \dot{q}_\Lambda(z)/H_0)$ pair for the concordance model can be computed from the formulae:

$$q_\Lambda(z) = \frac{3}{2}\Omega_m(z) - 1\,; \quad \frac{\dot{q}_\Lambda(z)}{H_0} = -\frac{3}{2}\,E_\Lambda(z)(1+z)\,\frac{d\Omega_m(z)}{dz} = -\frac{9}{2}E_\Lambda(z)\Omega_m(z)\,[1-\Omega_m(z)]\;, \tag{4.2}$$

where

$$\Omega_m(z) = \frac{\rho_m(z)}{\rho_c(z)} = \frac{\Omega_m^0(1+z)^3}{E_\Lambda^2(z)}\,; \qquad E_\Lambda(z) = \frac{H_\Lambda(z)}{H_0} = \sqrt{\Omega_m^0(1+z)^3 + 1 - \Omega_m^0}\;. \tag{4.3}$$

Therefore, for $\Omega_m^0 = 0.27$ we obtain $(q_{0\Lambda}, \dot{q}_{0\Lambda}/H_0) \simeq (-0.595, -0.887)$, as quoted in the first row of Table 1. Let us mention that we have checked that using the earlier SNIa results (UNION) of Kowalski et al. [39] does not change significantly the previously presented constraints. Finally, let us clarify that the chosen initial value $\rho_\Lambda^i = -10^{60}\,\rho_c^0$ for the vacuum energy is completely arbitrary and the results do not depend on it because the relaxation mechanism is dynamical and hence works for any numerical choice of ρ_Λ^i. However, in order to avoid instabilities in the lengthy numerical analysis involved in the solution of these models (in which the large quantity ρ_Λ^i almost cancels against the dynamically generated numerical value of ρ_F) it is convenient not to choose ρ_Λ^i exceedingly large, but apart from this proviso any other arbitrarily selected value would do, as we have checked.

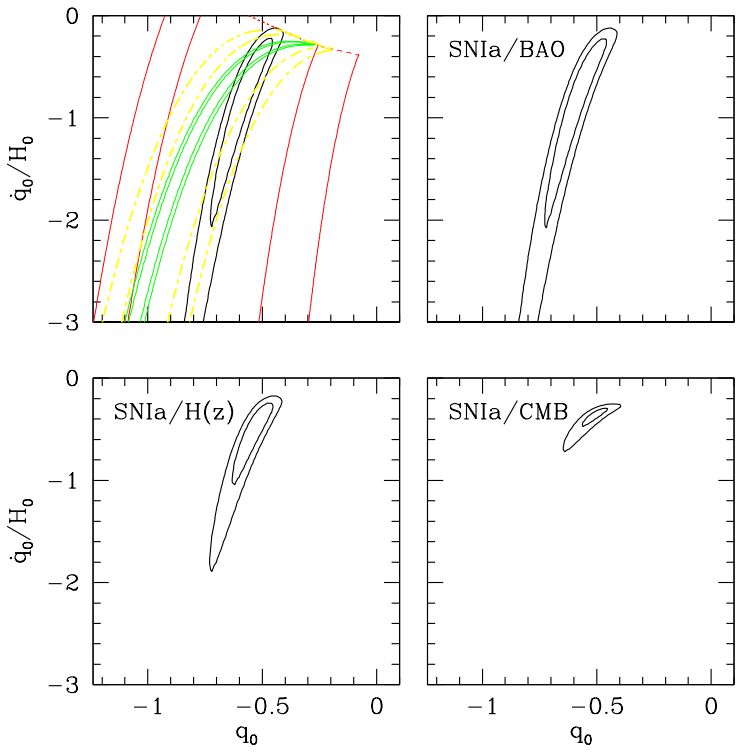

Figure 3: F_1^1 *model:* The Likelihood contours in the $(q_0, \dot{q}_0/H_0)$ plane. The different observational data are represented by different line types (see caption of Fig. 1 for definitions).

5. The expansion history/future for the F_m^n models

Since the current main cosmological quantities (scale factor, Hubble function etc.) exhibit a complicated scaling with the redshift, the absorption of the extra effects from the relaxation model into an "effective dark energy" contribution, with a non-trivial EoS of the form $\omega_{\rm eff}(z) = p_{\Lambda{\rm eff}}(z)/\rho_{\Lambda{\rm eff}}(z)$ is possible with the effective pressure $p_{\Lambda{\rm eff}}(z)$ and energy density $\rho_{\Lambda{\rm eff}}(z)$ taken from Eqs. (2.5). The corresponding EoS for the matter component is not affected by the presence of the F-term, so that the behavior of the matter epoch is the expected one. Indeed, during the background evolution in e.g. the non-relativistic matter dominated era, the deceleration parameter q changes only very slightly to compensate the decreasing Hubble rate $H \sim t^{-1}$, but q always stays around the value $\frac{1}{2}$. Therefore, the universe expands like a matter dominated cosmos despite $|\rho_\Lambda^i| \gg \rho_m$. Analogously, q will vary minimally around the value 1 to ensure $|\rho_{\Lambda{\rm eff}}| \ll |\rho_\Lambda^i|$ during the radiation regime. Eventually, in the asymptotic future the relaxation of the CC is guaranteed by the smallness of H in the function B (2.10) at late times. The correct temporal sequence of the three cosmic epochs follows from the different powers of H in the function B, where higher powers are more relevant at earlier times: $\sim H^6$ for the radiation dominated epoch, and $\sim H^4$ for the matter and vacuum dominated epochs, although for the latter H becomes smaller than in the former because q is no longer close to 1/2. As we can see, all these dynamical features

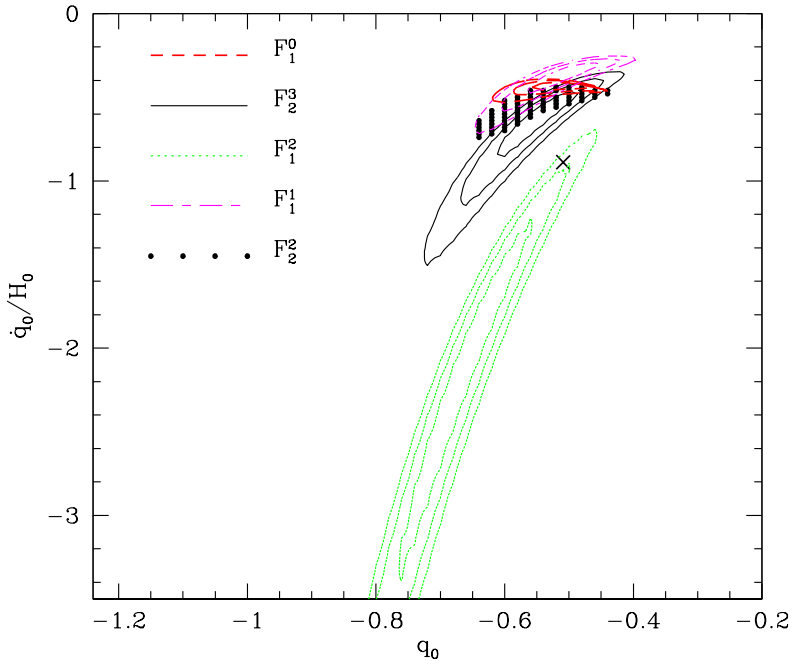

Figure 4: The overall Likelihood contours in the $(q_0, \dot{q}_0/H_0)$ plane, computed from (3.9). The contours are plotted where $-2\ln(\mathcal{L}/\mathcal{L}_{\max})$ is equal to 2.32, 6.16 and 11.83, corresponding to 1σ, 2σ and 3σ confidence level. The different F_m^n cosmological models are represented by the following types: F_1^0 red dashed line, F_2^3 black solid line, F_1^2 green dotted line and F_2^2 black dotted area (see Table I). For comparison, the cross corresponds to the traditional ΛCDM model.

are encoded in the structure of (2.10). The precise behavior of the relevant quantities in the various epochs becomes transparent in the various numerical examples considered in this section (cf. Figs. 5 and 6), on which we will elaborate further below).

In general, it is well known that one can express the effective dark energy EoS parameter in terms of the Hubble rate, $H(z)$. This function of the cosmological redshift z becomes known (numerically) after we explicitly solve the model as indicated in Sect. 4. In the present case the structure of the effective EoS of the DE is quite cumbersome. First of all, from the formulae of Sect. 2 one can show that

$$\omega_{\rm eff}(z) = \frac{p_{\Lambda{\rm eff}}(z)}{\rho_{\Lambda{\rm eff}}(z)} = -1 + [1+\omega_F(z)]\,\frac{\rho_F(z)}{\rho_\Lambda^i + \rho_F(z)} = -1 + 2\,\frac{E_0^0(z) - \frac{1}{3}\,E_i^i(z)}{\rho_\Lambda^i + 2\,E_0^0(z)}\,, \qquad (5.1)$$

where

$$\omega_F(z) = \frac{p_F(z)}{\rho_F(z)} = -\frac{1}{3}\,\frac{E_i^i(z)}{E_0^0(z)}\,. \qquad (5.2)$$

In view of equations (2.3) and (2.4), the previous expressions are complicated functions of z. From (5.1) and (5.2) it is patent that if we would have $E_0^0 = (1/3)\,E_i^i$, then the EoS

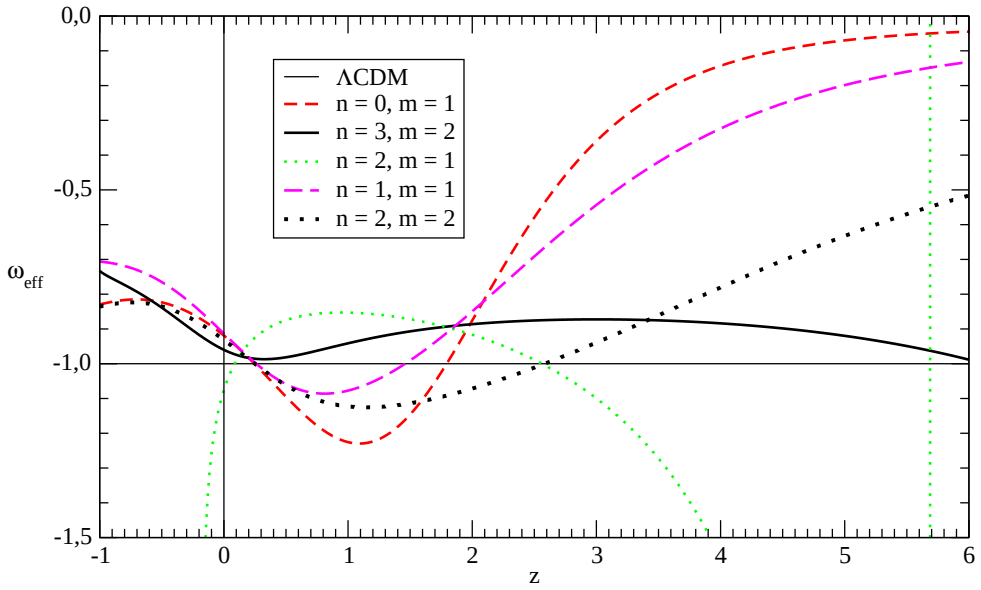

Figure 5: The effective equation of state $\omega_{\rm eff}$ as a function of the redshift z for the F_m^n models with initial conditions taken from Table 1 and with $\Omega_m^0 = 0.27$. The horizontal line $\omega_{\rm eff} = -1$ corresponds to the ΛCDM model.

of the induced DE density would be $\omega_F = -1$, and at the same time the EoS of the measurable effective vacuum energy would also be $\omega_{\rm eff} = -1$. However, as we can see from equations (2.3) and (2.4), the relation $E^0_{\ 0} = (1/3)\, E^i_{\ i}$ is only satisfied by the F-terms on the respective *r.h.s.* of these equations, but not by the remaining terms. Therefore, the effective EoS of the measurable DE density is expected to have a non-trivial behavior, and we must check if this behavior is still sufficiently close to the ΛCDM result $\omega_\Lambda = -1$, particularly at $z = 0$, and also determine what is its behavior as a function of the redshift.

In order to visualize the redshift dependence of the effective EoS parameter, we compare in Fig. 5 the various F_m^n cosmological models indicated in Table I of Sect. 4. One can divide the evolution of the cosmic expansion history in different phases on the basis of the varying behavior of the F_m^n and ΛCDM models. We will investigate such variations in terms of the deceleration parameter, $q(z) = -1 + d(\ln H)/d(\ln(1+z))$, which is plotted in Fig. 6. Below we briefly present the cosmic expansion history of the F_m^n models studied here. Note that we always compare with the concordance ΛCDM cosmology.

Although we do not focus here on the details of the radiation dominated period within our model, let us recall that it has been discussed in Sect.5.2 of Ref. [11]. From the approximate effective equation of state of the radiation epoch – see eq.(5.8) of that reference – one can see that it behaves radiation-like, i.e. $\omega_{\rm eff} \simeq 1/3$, and smoothly connects with $\omega_{\rm eff} \simeq 0$ in the matter dominated epoch during equality. Therefore the behavior is perfectly compatible with that of the ΛCDM model. This is corroborated by the numerical solution of the full field equations [11]. Finally, we point out that there is no significant effect that could alter the BBN phase of the radiation epoch because, as indicated previously, the form (2.9)-(2.10) insures that the dynamical relaxation mechanism automatically reduces

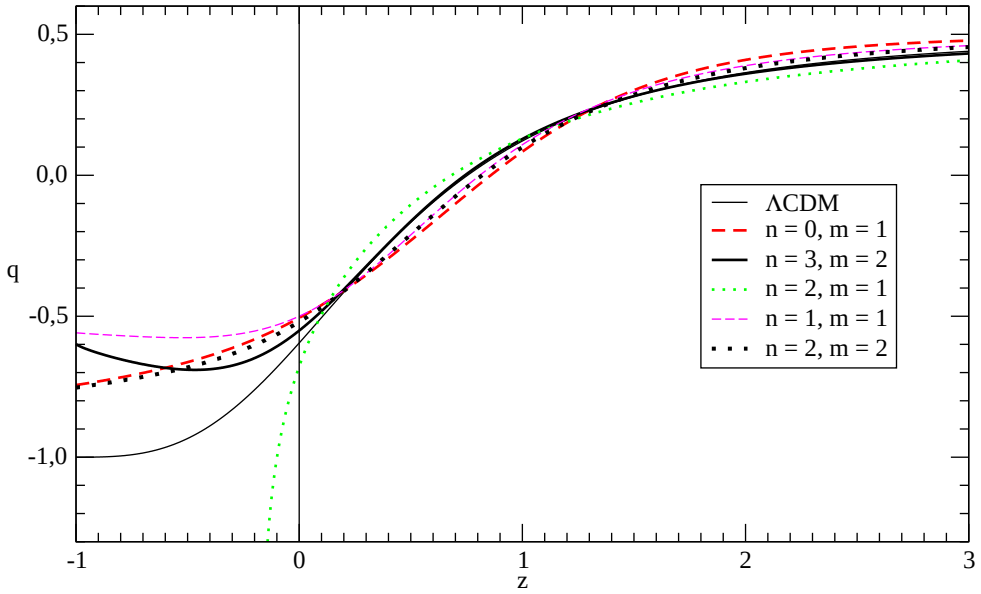

Figure 6: The deceleration factor $q(z)$ as a function of the redshift z for the ΛCDM model with $\Omega_m^0 = 0.27$ and for the F_m^n models with initial conditions taken from Table 1. Note that for $z > 0.2$ the curves of the models ΛCDM and F_2^3 are overlapping.

the big initial CC to a tiny value at all epochs, starting from the radiation epoch, going through the matter epoch until our present epoch. The density of vacuum energy during BBN therefore was completely subdominant and could not have any measurable effect on the standard light element abundances.

Prior to the radiation epoch we have the inflationary epoch. The latter should not be affected by the relaxation mechanism. This can be seen once more from the general structure of the functional (2.9)-(2.10). In the inflationary epoch, H is very large and q is near -1. Therefore the behavior of F in equation (2.9) is of the form $F \sim 1/H^{6m-2n}$, which after applying the natural relaxation condition (2.17) implies it is severely suppressed as $|F| \leq 1/H^{2m}$, at least. Thus, the universe is then completely controlled by the physics of the inflationary epoch, whatever it be, without receiving any interference from our relaxation mechanism. This mechanism only starts working when the universe leaves the inflationary epoch and enters the radiation dominated one, since then $q \to +1$ and this triggers the first large contribution from F that compensates for the value of the huge CC left over at the end of the inflationary period. Although we do not attempt to describe here how the inflationary epoch transited into the radiation dominated one, in the original formulation of the relaxation model [4] it was suggested that the functional F in equation (2.9) could contain an additive polynomial $A(R)$ of the Ricci scalar. In its simplest non-trivial form it would just entail a term proportional to R^2, which would not alter the relaxation mechanism in the radiation epoch. The advantage of this addition is that it could connect this relaxation model with a Starobinsky's type of mechanism for inflation [40] and subsequent modifications thereof, see e.g. [41] and references therein.

5.1 Cosmic acceleration and effective EoS analysis

In the following, we remark some features that can be observed from the behavior of the effective EoS and deceleration parameter of the various relaxation models under consideration in Figs. 5 and 6, respectively:

- F_1^0 **model:** For $z \geq 1$ the deceleration parameters (both for F_1^0 and ΛCDM) are positive with $q(z) \gtrsim q_\Lambda(z)$, which means that the cosmic expansion in the F_1^0 model is more rapidly "decelerating" than in the ΛCDM case. At $z \sim 0.8$ both models are starting to accelerate. Between $0.2 \lesssim z \lesssim 0.8$ the deceleration parameters are both negative with $q(z) < q_\Lambda(z)$. Now we will focus on the evolution of the effective EoS parameter. In particular, we find that at early enough times $z \geq 3$ the effective EoS parameter $\omega_{\rm eff}(z)$ of the F_1^0 model approaches zero [8], while we always have $\omega_\Lambda(z) = -1$ for the ΛCDM model. At $z \simeq 1.8$ the F_1^0 effective EoS parameter crosses the phantom divide line ($\omega_{\rm eff} = -1$) and it stays there for some time ($0.2 \lesssim z \lesssim 1.8$). Close to the present epoch, the effective EoS parameter crosses the phantom divide again and it behaves quintessence-like at present, where $\omega_{\rm eff}(0) \simeq -0.92$. In the future, it sustains this quintessence-like behavior and tends to $\omega_{\rm eff}^\infty \simeq -0.83$.

- F_1^1 **model:** this case behaves qualitatively very similarly to the F_1^0 model with a transient $\omega_{\rm eff} < -1$ phase in the past and quintessence like behavior in the asymptotic future. It also behaves quintessence-like at $z = 0$, where it takes essentially the same value of $\omega_{\rm eff}(0) \simeq -0.91$ as in the previous model. The asymptotic EoS behavior is $\omega_{\rm eff}^\infty \simeq -0.6$.

- F_2^3 **model:** for $0 \leq z \leq 3$ the deceleration parameter practically coincides with that of the concordance Λ cosmology, which means that the cosmic expansion in the F_2^3 model mimicks that of the ΛCDM case. Also, the effective EoS is not far from -1 in this region, but it stays above the phantom divide line. Specifically, the current value is $\omega_{\rm eff}(0) \simeq -0.96$. For $z < 0$ (future) the deceleration parameters are both negative with $q(z) > q_\Lambda(z)$, which means that the cosmic expansion in the ΛCDM model is more rapidly "accelerating" than in the F_2^3 case. The latter approaches a quintessence like future with $\omega_{\rm eff}^\infty \simeq -0.73$.

- F_1^2 **model** (or "no-scale" model): for $1 \leq z \leq 3$ the deceleration parameter remains close to that of the concordance Λ cosmology. Then at $z \sim 0.7$ both models are starting to accelerate and between $0 \lesssim z \lesssim 0.7$ the deceleration parameters are both negative with $q(z) > q_\Lambda(z)$. Near the present epoch, the effective EoS parameter $\omega_{\rm eff} \sim -1$, in particular the current value is $\omega_{\rm eff}(0) \simeq -1.08$. Interestingly, in the future the F_1^2 leads to an apparent singularity ($\omega_{\rm eff}(z) \ll -1$) caused by the pole that $\omega_{\rm eff}$ has at $z \sim 5.7$ due to $\rho_{\Lambda{\rm eff}}$ changing its sign. There is, however, no physical divergence related to it because all energy densities remain finite. The dramatic change of qualitative behavior of this model with respect to the others is nevertheless

[8] This is no surprise, it is actually a common feature expected for general ΛXCDM models (as the relaxation models indeed are), see [13] for details.

remarkable. In particular, the fact that F_1^2 behaves mildly phantom-like at present could explain the persistent tilt of the EoS data pointing slightly below -1 at $z = 0$, if eventually confirmed by the observations.

- F_2^2 **model:** close to the present time and in the future this model performs very similarly to the F_1^0 model with $\omega_{\rm eff}(0) \simeq -0.93$. However, the transient $\omega_{\rm eff} < -1$ phase between $z \approx 0.3$ and $z \approx 2.5$ started earlier in the past, roughly at the same redshift where the F_1^2 model switched from the phantom- to the quintessence-like EoS.

5.2 Phase space analysis for the "no-scale" models

The "no-scale" models $n = 2m$, like the F_1^2 discussed in the previous section, deserve a closer attention. From the peculiar structure of (2.20), we see that ρ_F is a function of only two arguments: $\rho_F = \rho_F(q, \dot{q}/H)$. This fact enables us to analyze the F_m^{2m} models in a $(q, \dot{q}/H)$ phase space diagram. This is generally not the case for the other models, for which ρ_F is in general a function of three (not just two) independent arguments $\rho_F = \rho_F(H, q, \dot{q}/H)$, see equation (2.18) and also Appendix A. If we focus once more on the canonical case F_1^2, we explicitly obtain

$$\rho_F(q, \dot{q}/H) = \frac{6\beta}{b^2}\left[(q^4 - 4q^3 + 9q^2 - 5q - 1) - (2q^3 - 6q + 5)\frac{\dot{q}}{Hb}\right], \tag{5.3}$$

with $\beta = M_X^4$ and b given by (2.19). If we compare with (2.18), here we have $f(q) = 6(q^4 - 4q^3 + 9q^2 - 5q - 1)/b^2$ and $g(q) = -6(2q^3 - 6q + 5)/b^3$, and from the value of q_0 taken by this model (see Table 1) we can see that $f(q_0)$ and $g(q_0)$ are of order 1 for that matter. The corresponding phase space diagram is depicted in Fig. 7. The background evolution follows mainly from $\rho_F + \rho_\Lambda^i = 0$, which yields $\dot{q}/H$ as a function of only q, see Fig. 7.

When $\dot{q}/H$ is very small, the deceleration does not change much. This happens around $q \approx \frac{1}{2}$ corresponding to the matter era. For smaller values of $q \lesssim \frac{1}{2}$, the time derivative $\dot{q}$ is negative and q will decrease with time. Finally, $\dot{q}$ will vanish again in another fixed point, which can be quintessence-like ($q > -1$) or phantom-like ($q < -1$), or $\dot{q}/H \to -\infty$ diverges at around $q \approx -2.05$. The type of final state depends on the value of $\rho_\Lambda^i/(2\beta)$ (the values are attached to the curves in Fig. 7) or equivalently on the current values of q_0 and $\dot{q}_0$. The smallness of the late-time Hubble rate H_0 results from the standard evolution of $H \approx \frac{2}{3}t^{-1}$ during the matter epoch, which corresponds to the unstable fixed point ($q = \frac{1}{2}$, $\dot{q} = 0$).

6. Conclusions

In this paper, we have confronted the class of modified gravity models of the form $F_m^n(R, \mathcal{G})$ – see equation (2.9) – with the main observational data. We have shown that the set of all models of this kind with $n \leq 2m$ are possible candidates capable to implement the dynamical relaxation of a large cosmological term, or vacuum energy density, irrespective of its value and size – typically $\rho_\Lambda^i \sim M_X^4$ (with $M_X \geq 10^{16}$ GeV). We have adopted the

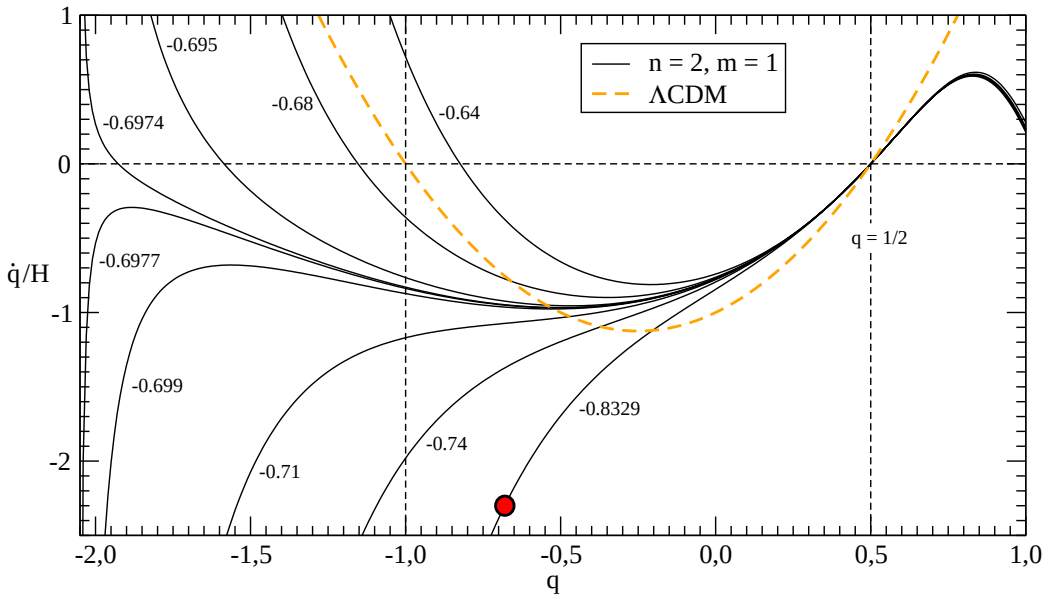

Figure 7: Phase space diagram for the case $n = 2$, $m = 1$. We plot $\dot{q}/H$ as a function of the deceleration q for different values of $\rho_\Lambda^i/(2\beta)$ (attached to the curves). The matter cosmos with $q = \frac{1}{2}$ (right vertical dashed line) is an attractor in the past. The red blob denotes the best-fit point ($q_0 = -0.68$, $\dot{q}_0 = -2.3$) found in the statistical analysis of Sect. 3. Moreover, we show $\dot{q}/H$ (dashed orange curve) for the ΛCDM model without radiation, which has also a stable fixed point at $q = -1$ corresponding to de Sitter space-time (left vertical dashed line). In this plot q is decreasing/increasing with time in the lower/upper part divided by the horizontal dashed line.

point of view that such a huge vacuum energy is an integral part of the energy budget of the universe, which was unavoidably deposited in it by the quantum fluctuations and the important phase transitions of the early times. All the usual modified gravity models we know of, and in fact most DE models of all kinds proposed in the literature, implicitly assume that this gigantic energy is just canceled by some extremely fine tuned counterterm such that the measured value is the tiny number $\rho_\Lambda^0 \sim 10^{-47}$ GeV^4 (in particle physics units), otherwise the cosmos could not evolve in the observed standard manner. Usually the measured value is then linked to some late-time effective gravity modification or to the residual value of some scalar field potential. However, the preposterous cancelation that was implicitly assumed to get rid of the huge initial vacuum energy density is generally recognized by theoretical physicists as completely unnatural and unacceptable.

Quite in contrast, the relaxation mechanism that we have put to the observational test in this paper is able to counterbalance the large vacuum energy (whatever its value and size) in a totally dynamical way (hence without any sort of fine tuning) thanks to an effective action which is modified by the presence of the $F_m^n(R, \mathcal{G})$ terms. By carefully comparing these relaxation models with the most recent observational data on SNIa, CMB, BAO and high redshift $H(z)$, we have shown in particular that the simplest candidates in the list, namely F_1^0, F_1^1, F_2^3, F_1^2 and F_2^2, can provide a background cosmic evolution very close to the concordance ΛCDM model. In other words, these F_m^n models yield a fairly standard-like

cosmological evolution going through the normal radiation dominated, matter dominated, and CC dominated epochs, they also exhibit an effective EoS behavior very near to -1 around $z = 0$, and finally (and this is of course the main point to be stressed here) they do all this without any need of enforcing fine tuning in order to get rid of the huge vacuum energy injected in the cosmos during the early stages of its evolution. In particular, the "no-scale" relaxation models, i.e. the entire class F_m^{2m}, can provide a natural relaxation of the vacuum energy without introducing any other energy scale except that of the vacuum energy itself. The other F_m^n models, with $n \neq 2m$, involve a mass scale which, for the canonical candidates mentioned above, is of the order of a typical Particle Physics scale in the SM of electroweak and strong interactions. Furthermore, in contrast to quintessence-like models, these relaxation models do not involve extremely tiny mass scales. Actually, the typical scales that are required are fixed in order of magnitude only, and therefore there is no need at all of exerting fine-tuning in any of the F_m^n models so as to dynamically reduce the huge initial value of the vacuum energy density $\rho_\Lambda^i \sim M_X^4$ into the very small one, $\rho_\Lambda^0 \sim 10^{-47}$ GeV^4, measured in our current universe. The class of models studied here can be thought of as a prototype for eventually solving the "old CC problem" without departing significantly from the expansion history of the concordance model. However, more realistic models are of course needed in order to provide a true solution to the cosmological constant problem from the point of view of fundamental physics.

Acknowledgments

This work has been supported in part by MEC and FEDER under project FPA2010-20807, by the Spanish Consolider-Ingenio 2010 program CPAN CSD2007-00042 and by DIUE/CUR Generalitat de Catalunya under project 2009SGR502. SB wishes to thank the Dept. ECM of the Univ. de Barcelona for the hospitality, and the financial support from the Spanish Ministry of Education, within the program of Estancias de Profesores e Investigadores Extranjeros en Centros Españoles (SAB2010-0118).

A. Computing ρ_F for the canonical models: $F_1^0, F_1^1, F_1^2, F_2^3, F_2^2$

Here we quote the explicit expressions for $\rho_F = 2E_0^0$ for our favorite F_m^n models in Table 1 of Sect. 4.2, which are obtained from explicit computation of (2.3). To avoid too lengthy expressions we set $y = 0$ in equation (2.10) as it is not important for the matter dominated epoch or any time after it, and in this way they all take the general form $\rho_F(H, q, \dot{q}/H)$ given in (2.18), with the notation (2.19). The explicit results read as follows:

1. Case $n = 0$, $m = 1$, with $|\beta| = \mathcal{M}^8$:

$$\rho_F = \frac{\beta}{2b^2H^4}\left[(5q^2 - 3q - 5) - (4q^2 - 10q + 7)\frac{\dot{q}}{Hb}\right]; \tag{A.1}$$

2. Case $n = 1$, $m = 1$, with $|\beta| = \mathcal{M}^6$:

$$\rho_F = \frac{\beta}{b^2H^2}\left[-\frac{3}{2}(4q^3 - 7q^2 + 2q + 4) + (4q^3 - 12q^2 + 18q - 11)\frac{\dot{q}}{Hb}\right]; \tag{A.2}$$

3. Case $n = 2$, $m = 1$, with $|\beta| = \mathcal{M}^4$ (see Sect. 2.2 for a detailed discussion of this special case):

$$\rho_F = \frac{6\beta}{b^2}\left[(q^4 - 4q^3 + 9q^2 - 5q - 1) - (2q^3 - 6q + 5)\frac{\dot{q}}{Hb}\right]. \tag{A.3}$$

4. Case $n = 3$, $m = 2$, with $|\beta| = \mathcal{M}^6$:

$$\rho_F = \frac{3(q-1)\beta}{b^3H^2}\Big[-3(q-1)(4q^3 - 6q^2 + 5q + 6) + (4q^4 - 12q^3 + 28q^2 - 36q + 19)\frac{\dot{q}}{Hb}\Big]; \tag{A.4}$$

5. Case $n = 2$, $m = 2$, with $|\beta| = \mathcal{M}^8$:

$$\rho_F = \frac{\beta}{8\,b^3H^4}\Big[(30q^4 - 73q^3 + 44q^2 + 37q - 38) - 2(12q^4 - 48q^3 + 88q^2 - 82q + 31)\,\frac{\dot{q}}{Hb}\Big]. \tag{A.5}$$

In all cases $\mathcal{M}$ is a mass scale associated to the relaxation mechanism, which depends on the particular model, see equation (2.14). The numerical value of that scale (fixed in order of magnitude only) is determined by the value of ρ^i_Λ. The models listed above have been chosen because they all satisfy the "natural relaxation condition" (2.17), and for all of them $\mathcal{M}$ takes a characteristic value which ranges from a mass scale of the SM of Particle Physics to the GUT scale associated the big initial value of the vacuum energy, $\rho^i_\Lambda \sim M_X^4$. See sections 2.1 and 2.2 for details.

References

[1] E. Komatsu *et al.* [WMAP Collaboration], Astrophys. J. Supl. **180** (2009) 330 [arXiv:0803.0547]; Astrophys. J. Supl. **192** (2011) 18 [arXiv:1001.4538].

[2] R. Knop et al., Astrophys. J. **598** (2003) 102 [arXiv:astro-ph/0309368]; A. Riess *et al.* Astrophys. J. **607** (2004) 665 [arXiv:astro-ph/0402512].

[3] S. Weinberg, Rev. Mod. Phys. **61** (1989) 1-23; V. Sahni, A. A. Starobinsky, Int. J. Mod. Phys. **D9** (2000) 373 [arXiv:astro-ph/9904398]; S. M. Carroll, Living Rev. Rel. **4** (2001) 1 [arXiv:astro-ph/0004075]; T. Padmanabhan, Phys. Rept. **380** (2003) 235 [hep-th/0212290].

[4] F. Bauer, J. Solà, H. Štefančić, *Dynamically avoiding fine-tuning the cosmological constant: The Relaxed Universe*, JCAP **1012** (2010) 029 [arXiv:1006.3944].

[5] P. J. E. Peebles, B. Ratra, Rev. Mod. Phys. **75** (2003) 559 [arXiv:astro-ph/0207347]; E. J. Copeland, M. Sami, S. Tsujikawa, Int. J. Mod. Phys. **D15** (2006) 1753 [hep-th/0603057]; S. Nojiri and S. D. Odintsov, Int. J. Geom. Meth. Mod. Phys. **4** (2007) 115 [hep-th/0601213]; M. Li, X. -D. Li, S. Wang, Y. Wang, Commun. Theor. Phys. **56** (2011) 525 [arXiv:1103.5870]; D. Saez-Gomez [arXiv:1104.0813].

[6] F. Bauer, J. Phys. Conf. Ser. **259** (2010) 012083 [arXiv:1010.1106].

[7] J. Solà, J. Phys. Conf. Ser. **283** (2011) 012033 [arXiv:1102.1815]; Fortsch. Phys. **59** (2011) 1108, and references therein.

[8] J. Grande, J. Solà, S. Basilakos, and M. Plionis, JCAP **08** (2011) 007 [arXiv:1103.4632].

[9] S. Basilakos, M. Plionis and J. Solà, Phys. Rev. **D80** (2009) 083511 [arXiv:0907.4555]; Phys. Rev. **D82** (2010) 083512 [arXiv:1005.5592].

[10] M. Maggiore, L. Hollenstein, M. Jaccard, E. Mitsou, [arXiv:1104.3797]; M. Maggiore, Phys. Rev. **D83** (2011) 063514, arXiv:1004.1782; Z.-X. Zhai, T.-J. Zhang, W.-B. Liu, JCAP **08** (2011) 019 [arXiv:1109.1661].

[11] F. Bauer, J. Solà, H. Štefančić, Phys. Lett. **B688** (2010) 269 [arXiv:0912.0677].

[12] F. Bauer, J. Solà, H. Štefančić, Mod. Phys. Lett. **A26** (2011) 2559 [arXiv:1105.1030].

[13] J. Grande, J. Solà and H. Štefančić, JCAP **08** (2006) 011 [arXiv:gr-qc/0604057]; Phys. Lett. **B645** (2007) 236 [arXiv:gr-qc/0609083]; J. Grande, A. Pelinson, J. Solà, Phys. Rev. **D79** (2009) 043006 [arXiv:0809.3462] and [arXiv:0904.3293] .

[14] S. Nojiri, S. D. Odintsov, Phys. Rev. D **72** (2005) 023003; H. Štefančić, Phys. Lett. **B670** (2009) 246.

[15] F. Bauer, J. Solà, H. Štefančić, Phys. Lett. **B678** (2009) 427 [arXiv:0902.2215]; F. Bauer, Class. Quant. Grav. **27** (2010) 055001 [arXiv:0909.2237].

[16] F. Bauer, Gen. Rel. Grav. **43** (2011) 1733 [arXiv:1007.2546]; Class. Quant. Grav. **28** (2011) 225019 [arXiv:1108.0875].

[17] A.D. Dolgov, in: *The very Early Universe*, Ed. G. Gibbons, S.W. Hawking, S.T. Tiklos (Cambridge U., 1982); L.F. Abbott, Phys. Lett. **B150** (1985) 427; L.H. Ford, Phys. Rev. **D35** (1987) 2339; R.D. Peccei, J. Solà and C. Wetterich, Phys. Lett. **B195** (1987) 183; S. M. Barr, Phys. Rev. **D36** (1987) 1691; J. Solà, Phys. Lett. **B228** (1989) 317; Int. J. of Mod. Phys. **A5** (1990) 4225.

[18] S. Nobbenhuis, Found. Phys. **36** (2006) 613-680 [arXiv:gr-qc/0411093]; S. M. Barr, S. -P. Ng, R. J. Scherrer, Phys. Rev. **D73** (2006) 063530 [hep-ph/0601053]; R. Erdem, J. Phys. A **A41** (2008) 235401 [arXiv:0712.2989]; [arXiv:1105.0345]; D. A. Demir, Found. Phys. **39** (2009) 1407 [arXiv:0910.2730]; Phys. Lett. **B701** (2011) 496 [arXiv:1102.2276]; N.C. Tsamis, R.P. Woodard [arXiv:1103.5134]; C. Charmousis, E. J. Copeland, A. Padilla, P. M. Saffin, [arXiv:1106.2000]; S. Aslanbeigi, G. Robbers, B. Z. Foster, K. Kohri, N. Afshordi [arXiv:1106.3955]; M. Hindmarsh, D. Litim, C. Rahmede, JCAP **07** (2011) 019 [arXiv:1101.5401]; A. Contillo, M. Hindmarsh, C. Rahmede, [arXiv:1108.0422]; R-J. Yang, [arXiv:1108.0227].

[19] D. J. Eisenstein et al. (SDSS Collab.), Astrophys. J., **633** (2005) 560 [arXiv:astro-ph/0501171]; N. Padmanabhan, et al. (SDSS Collab.), Mon. Not. Roy. Astron. Soc., **378** (2007) 852 [arXiv:astro-ph/0605302].

[20] D. Stern, R. Jiménez, L. Verde, M. Kamionkowski, S.A. Stanford, JCAP **02** (2010) 008 [arXiv:0907.3149].

[21] S. M. Carroll, A. De Felice, V. Duvvuri, D. A. Easson, M. Trodden, and M. S. Turner, Phys. Rev. **D71** (2005) 063513 [arXiv:astro-ph/0410031].

[22] S. Nojiri and S.D. Odintsov, eConf **C0602061** (2006) 06 [Int. J. Geom. Meth. Mod. Phys. **4** (2007) 115]; T.P. Sotiriou, V. Faraoni, Rev. Mod. Phys. **82** (2010) 451, arXiv:0805.1726 [gr-qc]; R. Woodard, *Lect. Notes Phys.* 720 (2007) 403 [arXiv:astro-ph/0601672]; S. Capozziello, M. De Laurentis [arXiv:1108.6266].

[23] K. Bamba, S. D. Odintsov, L. Sebastiani, and S. Zerbini, Eur. Phys. J **C67** (2010) 295 [arXiv:0911.4390].

[24] I. Navarro and K. van Acoleyen, JCAP **0603** (2006) 008 [arXiv:gr-qc/0511045]; D. Comelli, Phys. Rev. **D72** (2005) 064018 [arXiv:gr-qc/0505088].

[25] S. Nojiri and S. D. Odintsov, Phys. Lett. **B631** (2005) 1 [arXiv:hep-th/0508049]; G. Cognola *et al.*, Phys. Rev. **D73** (2006) 084007 [arXiv:hep-th/0601008]; Phys. Rev. **D75** (2007) 086002 [arXiv:hep-th/0611198].

[26] I. Navarro, and K. Van Acoleyen, Phys. Lett. **B622** (2005) 1 [arXiv:gr-qc/0506096].

[27] M. Hicken et al., Astroplys. J., **700** (2009) 1097 [arXiv:0901.4804].

[28] M.L. Tong, H. Noh, Eur. Phys. J **C71** (2011) 1586 [arXiv:1102.3254]; J. Lu, L. Xu, M. Liu, Phys. Lett. **B699** (2011) 246 [arXiv:1105.1871]; Y. Chen, B. Ratra [arXiv:1106.4294]; J.C. Fabris, P.L.C. de Oliveira, H.E.S. Velten [arXiv:1106.0645]; S. Cao, N. Liang, Z.H. Zhu [arXiv:1105.6274]; R.-G. Cai, Z.-L. Tuo [arXiv:1105.1603]; S. Lee [arXiv:1105.0993].

[29] W. J. Percival, Mon. Not. Roy. Astron. Soc., **401** (2010) 2148 [arXiv:0907.1660].

[30] J. R. Bond, G. Efstathiou and M. Tegmark, Mon. Not. Roy. Astron. Soc. **291** (1997) L33 [arXiv:astro-ph/9702100].

[31] S. Nesseris and L. Perivolaropoulos, JCAP **0701** (2007) 018 [arXiv:astro-ph/0610092].

[32] O. Elgarøy, T. Multamäki, Astron. Astrophys. **471** (2007) 65 [arXiv:astro-ph/0702343]; P.S. Corasaniti & A. Melchiorri Phys. Rev. D, **77** (2008) 103507.

[33] M. Plionis, P. Coles and P. Catelan, Mon. Not. Roy. Astron. Soc., **262** (1993) 465.

[34] A. G. Sanchez, C. M. Baugh, W. J. Percival, J. A. Peacock, N. D. Padilla, S. Cole, C. S. Frenk and P. Norberg, Mon. Not. Roy. Astron. Soc., **366** (2006) 189 [arXiv:astro-ph/0507583].

[35] H. Feldman *et al.*, Astrophys. J. Lett., **596** (2003) L131 [arXiv:astro-ph/0305078].

[36] R. Mohayaee, R.B. Tully, Astrophys. J., **635** (2005) L113 [arXiv:astro-ph/0509313].

[37] H. Andernach, M. Plionis, O. Lopez-Cruz and E. Tago, S. Basilakos, 2005, Astronomical Society of the Pacific Conference Series, **329** (2005) 289 [arXiv:astro-ph/0407098].

[38] S. Schindler, Space Science Reviews, **100** (2002) 299.

[39] M. Kowalski, et al., Astrophys. J., **686** (2008) 749 [arXiv:0804.4142].

[40] A.A. Starobinski, Phys. Lett. **B91** (1980) 99; A. Vilenkin, Phys. Rev. **D32** (1985) 2511.

[41] J. Solà, J. of Phys. **A41** (2008) 164066, arXiv:0710.4151 [hep-th].